ARTICLE

Crystal Structure and Magnetic Property of 2-(Imidazo[1,2-a]pyri-din-2-yl)-2-oxoacetic Acid and Its Perchlorate

Chen Shen, Yi-man Zhang, Guo-ping Yong*

Department of Chemistry, University of Science and Technology of China, Hefei 230026, China

We herein report two crystals based on 2-(imidazo[1,2-a]pyridin-2-yl)-2-oxoacetic acid radical and its perchlorate, and investigate the relationship between magnetic properties and crystal stacking structures or supramolecular interactions. 2-(imidazo[1,2-a]pyridin-2-yl)-2-oxoacetic acid radical in two crystals mainly exist as diamagnetic dimer formed via short atomic contacts or supramolecular interactions (hydrogen bonds, anion-π or lone-pair-π interactions), leading to low magnetic susceptibilities. 2-(imidazo[1,2-a]pyridin-2-yl)-2-oxoacetic acid radical crystal exhibits quasi-one-dimensional columnar stacking chain and weak antiferromagnetism. However, its perchlorate crystal possesses one-dimensional double-stranded chain structure assembled through double hydrogen bonds and anion-π interactions, and reveals weak ferromagnetism.

Key words: 2-(Imidazo[1,2-a]pyridin-2-yl)-2-oxoacetic acid radical, Crystallographic structure, Magnetic properties, Organic compound

I. INTRODUCTION

Organic crystals can exhibit many interesting properties including luminescence [1, 2], nonlinear optical [3, 4], or magnetic [5, 6] properties, *etc.* Therefore, developing organic crystal materials with advantages of light-weight, flexible, low-cost, and environmentally benign characteristics is in increasing demand, yet needs elaborate chemical designs and/or supramolecular interactions for objective functions. The supramolecular assembling process using non-covalent interactions such as hydrogen bond, π-π stacking, short atomic contact, lone-pair-π, and ion-π interaction, *etc.*, has been recognized as a high-potential technique to construct functional crystal materials. Amongst, the hydrogen bond is an important tool for creation of desired molecular arrangements and interesting properties. For example, hydrogen bond can behave as magnetic coupler of the organic radicals, giving rise to interesting magnetic organic materials [7, 8]. It is clear that the stacking of molecules via supramolecular interactions in the crystal structure is necessary for the successful design of molecular magnetic materials [9]. In order to exploit interesting and useful magnetic properties, the arrangement of the radical molecules in the solid state must be controlled, which is still a challenging issue. The progress in the development of radicals as molecular materials is strongly dependent upon the ability to control the structure at both the molecular and supramolec-

ular levels. For example, the thiazyl radicals exhibit strong supramolecular interactions in the crystal structures which lead to many interesting magnetic properties [10−14].

We are interested in the magnetic properties of 2, 3′-biimidazo[1,2-a] pyridin-2′-one (Hbipo$^{-\cdot}$) radical and its derivatives [15, 16]. Recently, we reported the magnetic properties based on 2-(imidazo[1,2-a]pyridin-2-yl)-2-oxoacetic acid radical [17]. In this work, we report the crystal structures and interesting magnetic properties of 2-(imidazo[1,2-a]pyridin-2-yl)-2-oxoacetic acid radical crystal A, and its perchlorate crystal B (HAClO$_4$). The interesting magnetic properties of radical crystals are relative to their crystal stacking structures and/or supramolecular interactions.

II. EXPERIMENTS

All commercial chemicals were used without further purification. The synthesis of 2-(imidazo[1,2-a]pyridin-2-yl)-2-oxoacetic acid (A) was previously described [2]. Single crystals of A·H$_2$O were grown by slow diffusion of acetone into the aqueous solution of A. Single crystals of B·H$_2$O were obtained by a slowly decreasing temperature (from 85 °C to room temperature) of perchloric acid aqueous solution (1:1, volume ratio) of A.

The crystal structures were studied by single crystal X-ray diffraction analysis using Gemini S Ultra CCD diffractometer (Oxford diffraction Ltd.), and the data were collected at 293(2) K by using graphite-monochromated Mo Kα radiation (λ=0.71073 Å) or Cu Kα radiation (λ=1.54184 Å). The crystal struc-

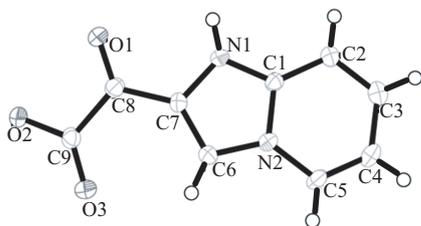*Author to whom correspondence should be addressed. E-mail: gpyong@ustc.edu.cn

FIG. 1 Molecular structure (thermal ellipsoids at 50% probability) and the atom numbering scheme for A·H_2O (water molecule omitted).

tures were solved by direct method and refined with full-matrix least-squares technique on structure factors F^2 by using the SHELXS-97 and SHELXL-97 programs. The EPR spectra were recorded on a JES-FA 200 ESR spectrometer at X-band. Temperature and field dependence of magnetic susceptibilities were measured for the microcrystalline samples using a SQUID magnetosusceptometer (Quantum Design MPMS).

III. RESULTS AND DISCUSSION

The crystallographic data and details of structure refinement have been reported [2,18]. All non-hydrogen atoms were refined anisotropically. The C−H hydrogen atom positions were geometrically generated and treated as riding on the heavier atoms to which they are attached, the N−H and O−H hydrogen atoms were located in the difference of Fourier maps and refined isotropically. Weighted residual factors R factor (R_w) and all goodness of fit (S value) are based on F^2, conventional factor R is based on F. The atom-numbering scheme for the crystal A·H_2O is shown in Fig.1. It is noticeable that A exists as an internal salt in the solid state [2], and it is a stable carboxyl radical [17], which can be demonstrated by its isotropic EPR signal with g-factor value of 2.005 (Fig.2). A·H_2O forms quasi-one-dimensional (1D) columnar stacking chain along the a-axis. In 1D chain, 2-(imidazo[1,2-a]pyridin-2-yl)-2-oxoacetic acid molecules adopt slipped anti-parallel stacking mode (Fig.3), in which there exist two kinds of short atomic contacts (C2···C2′ of 3.274 Å and C1···C1′ of 3.397 Å, shorter than van der Waals contacts) between neighboring molecules. It is noticeable that one short atomic contact of 3.274 Å results in head-to-head dimer structure which then forms quasi-1D chain through another short atomic contact of 3.397Å (Fig.3).

The atom-numbering scheme for the crystal B·H_2O is shown in Fig.4. As shown in Fig.5, radical molecules in B·H_2O exhibit largely slipped head-to-head dimer structure assembled by multiple hydrogen bonds at different temperatures (The hydrogen bonds of O8(water)-O4(perchlorate), O8(water)-O5(perchlorate), O8(water)-O3(carboxylic acid), and
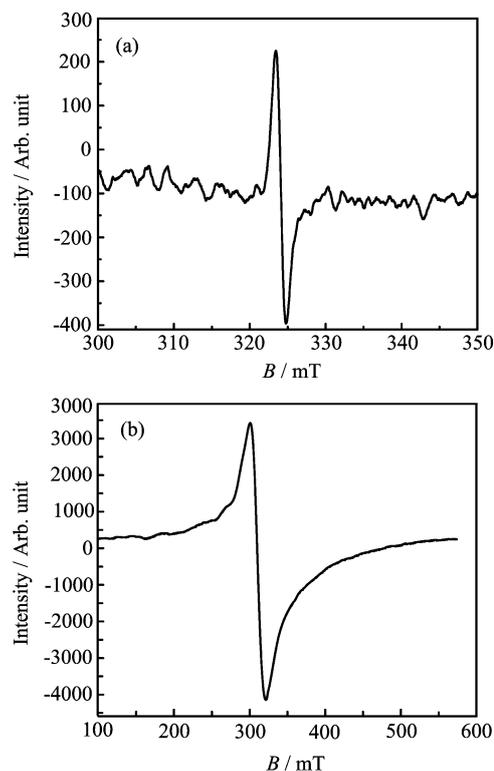

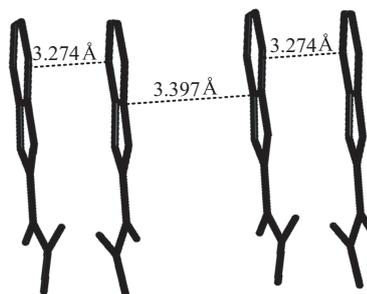FIG. 2 Solid-state EPR specta of (a) A·H_2O and (b) B·H_2O at room temperature.

FIG. 3 The columnar stacking chain in A·H_2O.

O5(perchlorate)-N2(imidazo[1,2-a]pyridine) are 2.969, 3.024, 2.562, and 2.965 Å at 293 K, while the hydrogen bonds are 2.893, 2.970, 2.545, and 2.940 Å at 150 K) and double lone-pair-π interactions between O8(water) and centroid (α-carbonyl acetic acid moiety) with centroid···O8 distance of 3.206 Å. The dimers form 1D double-stranded chain structure assembled through double anion-π interactions between O(perchlorate) and centroid (imidazo[1,2-a]pyridinium moiety) with centroid···O distance of 3.238 Å (Fig.5).

As shown in Fig.6, variable temperature SQUID measurement (1 kOe, 4−350 K) on the microcrystalline sample of A·H_2O shows that product of molar magnetic susceptibility and temperature $\chi_M T$ at 300 K is 0.038 emu·K/(Oe·mol), just 10% of that expected for
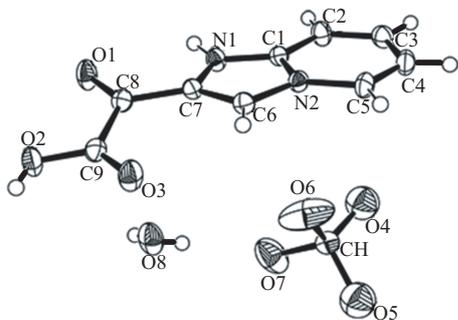
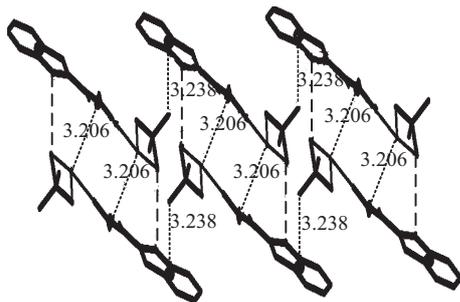FIG. 4 Molecular structure (thermal ellipsoids at 50% probability) and the atom numbering scheme for B·H_2O.

FIG. 5 Dimers and 1D double-stranded chain structure in B·H_2O formed by hydrogen bonds (dashed lines), and lone-pair-π and anion-π interactions (dotted lines).
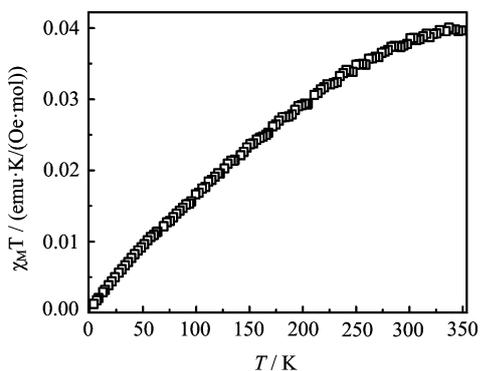

FIG. 6 Temperature dependence of $\chi_M T$ (field-cooled) for A·H_2O.

FIG. 7 Field dependent magnetization for A·H_2O at 5 K in the magnetic field ranges of ±10 kOe.
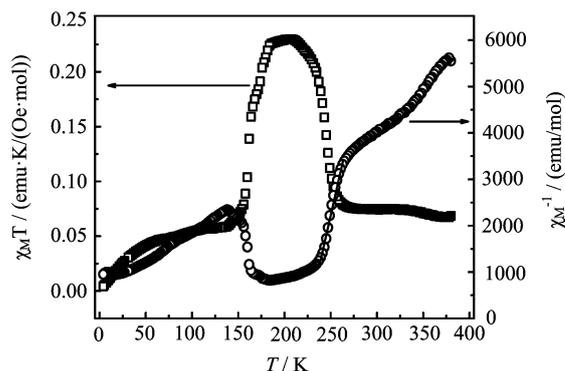
FIG. 8 Plots of $\chi_M T$ and χ_M^{-1} *vs.* T for B·H_2O. Solid line represents the best-fit curve.

an $S=1/2$ paramagnet, demonstrating the existence of diamagnetic dimers as described in crystal structure. Upon cooling from 350 K, the $\chi_M T$ gradually decreases to zero at 4 K, indicating a weak antiferromagnetic interaction between radicals, and the weak antiferromagnetic interaction of A·H_2O is relative to its dimer and quasi-1D chain structure. The field-dependent magnetization (M-H) curves at 5 K are shown in Fig 7. The M-H curves were obtained after correcting the original data for the contributions from the substrate and the background linear diamagnetic term. Such correction was also performed for compound B·H_2O. The magne-
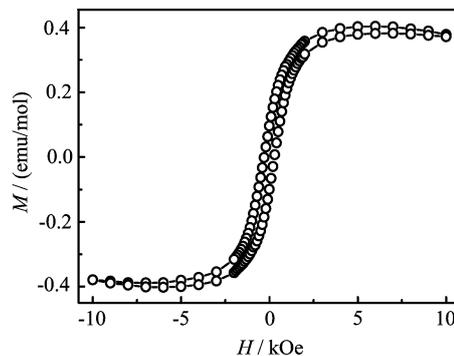
tization curve indicates an S-shaped curvature, and the magnetic hysteresis was observed with remnant magnetization M_r of about 0.12 emu/mol and coercive field H_c of about 278 Oe.

As shown in Fig.8, variable temperature SQUID measurements (1 kOe, 4−380 K) on the microcrystalline sample of B·H_2O show that $\chi_M T$ at 300 K is 0.075 emu·K/(Oe·mol), just 20% of that expected for an $S=1/2$ paramagnet, also indicating some extent diamagnetic dimers in B·H_2O as described by crystal structure. Interestingly, a dramatic surge in $\chi_M T$ takes place below 270 K with $\chi_M T$ reaching a broad maximum value of 0.232 emu·K/(Oe·mol) at about 220 K. This response indicates that B·H_2O may behave as a weak ferromagnetism [19]. At temperatures below 186 K, $\chi_M T$ value drops rapidly to 0.058 emu·K/(Oe·mol) at 138 K, and then slowly decreases to zero at 4 K. The data between 239 and 265 K for B·H_2O can fit to the Curie-Weiss expression with θ=222.5 K and a Curie constant C=0.012 emu/mol (Fig.8), indicative of a ferromagnetic coupling [20]. The cooling and warming measurements of susceptibility show no thermal hysteresis loop in the range of 4−380 K (Fig.9), indicating there is no magnetic phase transition in B·H_2O sample.

The field-dependent magnetization curve of B·H_2O indicates an S-shaped curvature even at room tempera-
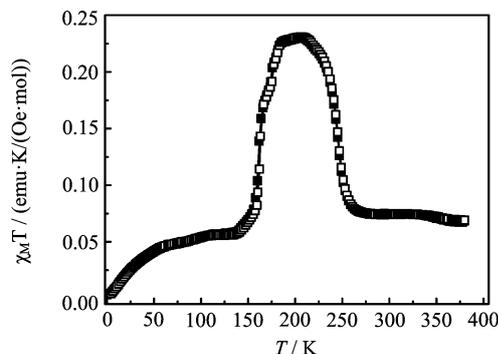
FIG. 9 Temperature dependence of susceptibility for B·H_2O, upon cooling (solid squares) and upon heating (open squares).

ture (300 K), as shown in Fig.10(a). In addition, a mild hysteresis is observed at 300 K (Fig.10(b)). These results substantiate that the sample is in a ferromagnetic state [21], although the accurate T_c value for B·H_2O is difficult to determine. Coercive field (H_c) and remanent magnetization (M_r) of B·H_2O at 300 K are about 75 Oe and 0.028 emu/mol, respectively. The magnetization curve at 5 K (Fig.10(c)) is almost the same as that at 300 K. Although the coercive field is larger (169 Oe). Moreover, compared to A·H_2O, B·H_2O shows a broad low field EPR signal with g value of 2.090 (Fig.(2b)), probably relative to its ferromagnetic behavior.

The reason of a ferromagnetic state in B·H_2O is not clear at present, however, the supramolecular interactions (hydrogen bonds, lone-pair-π, and anion-π interactions) might play an important role. Upon determining crystal structure of B·H_2O at 293 and 150 K, respectively, a slight increase in hydrogen bonding interactions at 150 K was observed, compared to at 293 K. Moreover, anion-π interactions (from 3.238 Å at 293 K to 3.133 Å at 150 K) and lone-pair-π interactions (from 3.206 Å at 293 K to 3.134 Å at 150 K) were also increased at low temperature. These changes of supramolecular interactions, especially anion-π interactions at different temperatures might induce the changes of the charge transfer and the intermolecular dipolar coupling and spin, giving rise to the ferromagnetic behavior.

IV. CONCLUSION

A neutral radical and its perchlorate crystals were successfully obtained, which mainly exist as diamagnetic dimers formed via short atomic contacts or supramolecular interactions (hydrogen bonds, anion-π or lone-pair-π interactions). The crystal stacking structures or supramolecular interactions lead to different magnetic behaviors. The crystal (A·H_2O) with quasi-1D columnar stacking chain exhibits weak antiferromagnetism, while, the crystal (B·H_2O) with 1D double-stranded chain structure assembled by hydrogen bonds
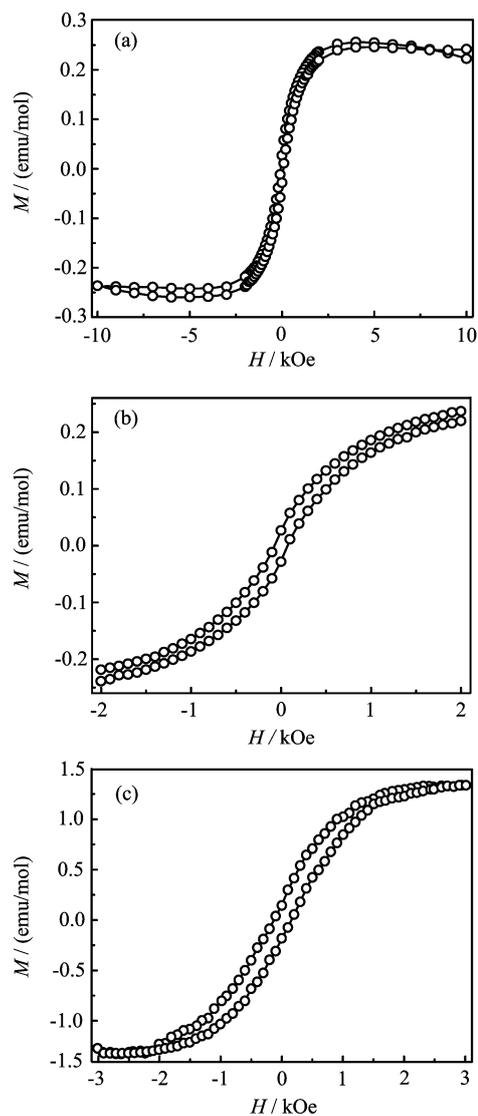

FIG. 10 Field dependent magnetization for B·H_2O at 300 K in the magnetic field ranges of (a) ±10 kOe and (b) ±2 kOe. (c) Magnetic hysteresis loop for B·H_2O at 5 K in the magnetic field ranges of ±3 kOe.

or anion-π interactions reveals weak ferromagnetism, because such supramolecular interactions can induce the changes of the charge transfer and the intermolecular dipolar coupling and spin, leading to the spin transfer to ferromagnetism. It is found that the unusual magnetic properties of radical crystals are intimately linked to their crystal stacking structures or supramolecular interactions.

V. ACKNOWLEDGMENTS

     ©2015 Chinese Physical Society

[1] O. Bolton, K. Lee, H. J. Kim, K. Y. Lin, and J. Kim, Nat. Chem. **3**, 205 (2011).

[2] G. P. Yong, Y. M. Zhang, W. L. She, and Y. Z. Li, J. Mater. Chem. **21**, 18520 (2011).

[3] T. L. Chen, Z. H. Sun, L. N. Li, S. Y. Wang, Y. Wang, J. H. Luo, and M. C. Hong, J. Cryst. Growth **338**, 157 (2012).

[4] T. Arumanayagam and P. Murugakoothan, J. Cryst. Growth **362**, 304 (2013).

[5] J. Takeda, M. Imae, O. Hanado, S. Kurita, M. Furuya, K. Ohno, and T. Kodaira, Chem. Phys. Lett. **378**, 456 (2003).

[6] W. A. Shelton, E. Aprà, B. G. Sumpter, A. Saraiva-Souza, A. G. Souza Filho, D. N. Jordan, and V. Meunier, Chem. Phys. Lett. **511**, 294 (2011).

[7] D. Maspoch, L. Catala, P. Gerbier, D. Ruiz-Molina, J. Vidal-Gancedo, K. Wurst, C. Rovira, and J. Veciana, Chem. Eur. J. **8**, 3635 (2002).

[8] L. M. Field and P. M. Lahti, Chem. Mater. **15**, 2861 (2003).

[9] D. A. Haynes, CrystEngComm **13**, 4793 (2011).

[10] W. Fujita and K. Awaga, Chem. Phys. Lett. **388**, 186 (2004).

[11] K. E. Preuss, Dalton Trans. 2357 (2007).

[12] J. M. Rawson, A. Alberola, and A. Whalley, J. Mater. Chem. **16**, 2560 (2006).

[13] W. Fujita and K. Kikuchi, Chem. Asian J. **4**, 400 (2009).

[14] S. M. Winter, K. Cvrkalj, P. A. Dube, C. M. Robertson, M. R. Probert, J. A. K. Howard, and R. T. Oakley, Chem. Commun. 7306 (2009).

[15] G. P. Yong, C. F. Li, Y. Z. Li, and S. W. Luo, Chem. Commun. **46**, 3194 (2010).

[16] Y. M. Zhang, G. P. Yong, C. F. Li, W. L. She, and Y. Z. Li, Synth. Met. **161**, 2708 (2012).

[17] G. P. Yong, Y. M. Zhang, and W. L. She, Mater. Lett. **92**, 358 (2013).

[18] G. P. Yong, Y. M. Zhang, and W. L. She, CrystEngComm **14**, 3923 (2012).

[19] K. L. Hu, M. Kurmoo, Z. M. Wang, and S. Gao, Chem. Eur. J. **15**, 12050 (2009).

[20] M. L. Taliaferro, M. S. Thorum, and J. S. Miller, Angew. Chem. Int. Ed. **45**, 5326 (2006).

[21] T. Sugimoto, K. Ueda, M. Tsujii, H. Fujita, N. Hosoito, N. Kanehisa, Y. Shibamoto, and Y. Kai, Chem. Phys. Lett. **249**, 304 (1996).